Second layer of ^{4}He on graphite

P.A. Whitlock

CIS Department, Brooklyn College
Brooklyn, NY 11210, USA

Badri Krishnamachari and G.V. Chester

Laboratory of Atomic and Solid State Physics, Cornell University
Ithaca, NY 14853

1. INTRODUCTION

In this report we present equations of state for the fluid and solid phases of the second layer of ^{4}He on a smooth graphite substrate studied by the Green's function Monte Carlo methods. Our reasons for conducting a careful study of the second layer are twofold. First the observation by Crowell and Reppy[1] that superfluidity exists in the second layer only over a well defined, and rather limited, range of densities, requires an explanation. It is not possible to account for these results if one treats the second layer as two dimensional (2D) helium[1]. Second, work on the second layer the first layer is often treated as static, and as producing an effective potential for the second layer atoms[2]. We wished to test this approach by treating both layers on an equal footing, that is, allowing the atoms in the first layer to fully participate in the simulation. The results of the latter calculation can be compared with those based on the effective potential approximation. To do this requires the development of a second layer energy estimator for the inhomogeneous system.

The first layer of helium on graphite is, when the second layer starts to form, a very dense almost two dimensional solid and the atomic motions are now quite limited. The mean square displacements, in the plane from the lattice sites are fairly small, about 6% of the nearest neighbor distance. The displacements out of the plane are also small; the first layer profile is only 0.7Å wide at half height. All of these facts suggest that treating the first layer as a passive entity is likely to be a fairly accurate approximation. We believe our comparison between a passive first layer and an active first layer is valuable because it should provide a guide of what to expect when one treats the third layer in the same way. The third layer lies over a low density solid second layer in which the atomic motions both in and out of the

plane are much larger than those of the first layer. The second layer is therefore very active and presumably more likely to be effected by the presence of the third layer. Superfluidity is seen in the third layer at very low densities[1], far below the density at which one might expect a homogeneous fluid to form. This surprising observation can only be explained by the interaction of the third layer with the very low density crystal phase of the second layer. Thus the dilute third layer poses a special simulation challenge.

2. PASSIVE EFFECTIVE POTENTIAL CALCULATIONS

This work is a continuation of our earlier work in which we obtained the equations of state for the first ^{4}He layer[3], hereafter called I. One approach for the second layer simulation is to view the underlying first layer as providing an effective potential for atoms in the second layer. This effective potential together with the potential from the carbon substrate provide a total potential to bind the helium atoms to the first layer. We have chosen to call the potential calculated in this way a passive effective potential (PEP). In the PEP used in our calculation, we treat the first layer as a two dimensional continuum. A preliminary report of the PEP results has been published[4] and they are in close agreement with those published by Pierce and Manousakis[5]. Pierce and Manousakis treated the first layer as a static two dimensional lattice. Our model is thus simpler and does not reveal the commensurate phases in the second layer. However we believe that a careful treatment of this simpler model is worthwhile because it will show which features of the equations of state depend on the presence of the corrugated substrate and which do not. In both cases an effective potential for atoms in the second layer was calculated using an Aziz two body potential[6].

The results of Pierce and Manousakis[5] were obtained for a smaller system (a maximum of 48 particles) by path integral (PI) simulations[7]. Our simulations used 96 to 108 atoms in the second layer. Since both methods, if well converged, should yield exact equations of state, it is important to have the results of both to compare. We should also note that each method also has its own special difficulties. Our results are based on the Green's function Monte Carlo (GFMC) method which relies on an accurate importance function for good convergence. It is conceivable that for the highly inhomogeneous film system that even a good importance function could bias the results. On the other hand, the PI method requires that one extrapolate finite temperature results to absolute zero to obtain ground state properties. This extrapolation can be uncertain because convergence can be difficult to achieve at low temperatures. The close agreement between the two methods provides conformation that both are correct.

Our methods for the second layer, based on the use of a PEP, are essentially the same as those we used in I for the first layer. The effective potential for an atom in the second layer, provided by the carbon substrate and the first layer of helium, has a well depth of approximately -50 K, whereas the carbon potential for the first layer has a well depth of -180 K. Thus the wave function of a single helium atom in the second layer is significantly wider (1.0 Å) as compared with that of an atom in the first layer (0.7 Å). We expect[3] the wider wave function will cause an increased

binding of the fluid in the second layer as compared with the first layer. The position of the 2D plane was centered on the peak of the wave function for the first layer.

Our variational wave function for the atoms in the second layer was a product of pair and triplet functions multiplied by a product of single particle functions, one for each atom. These single particle functions were taken to be the ground state of a single atom in the effective potential provided by the carbon substrate and the first layer. The forms for the two and three body pseudopotentials were the same as before; see equations 5 – 7 of I. At each density the parameters in this wave function were optimized to give the lowest energy for the system. This optimized wave function was then used as an importance function in a GFMC calculation.

We fitted our energies to the same polynomial forms as a function of density, ρ, that we used previously:

$$E = E_o + B\left(\frac{\rho - \rho_o}{\rho_o}\right)^2 + C\left(\frac{\rho - \rho_o}{\rho_o}\right)^3 . \tag{1}$$

From these equations we were able to make a Maxwell double tangent construction to determine the freezing and melting densities. The value of ρ_0, 0.0477Å^{-2}, in the fluid phase is the density at which the pressure is zero. At lower densities the system will form almost two dimensional puddles which need not be connected. Our value of ρ_0 is the same as that found by Pierce and Manousakis[5], 0.048Å^{-2}. Thus our PEP value is very close to the lower limit in density, 0.05Å^{-2}, for which Crowell and Reppy observed superfluidity in the second layer[1]. It is possible that the same calculation, but using the most recent Aziz two body potential[8] might still further increase the value of ρ_0. It is unlikely, because of the comparatively low density represented by ρ_0, that the introduction of a three body potential will have an significant effect. The value of the PEP freezing density, 0.07Å^{-2}, is also interesting in the light of the superfluity experiments. Crowell and Reppy found that the maximum density for superflow in the second layer was approximately 0.07Å^{-2}. The simulation value of 0.07Å^{-2} is still somewhat uncertain, due to approximations in the model, and the actual value may well be lower. If this is the case then the experimental upper limit will lie in the two phase, solid-liquid, region. Patches of solid have now formed and are disrupting the superflow.

3. FULL PARTICIPATION OF THE FIRST LAYER ATOMS

We now turn to the calculation in which both the first and second layers are treated on an equal footing. Our Hamiltonian is now given by;

$$H = H_1 + H_2 + V_{12} . \tag{2}$$

Where H_1 and H_2 are the Hamiltonians for two groups of helium atoms interacting with the carbon substrate, N_1 in the first layer and N_2 in the second layer. At the outset it is useful to identify these two distinct groups of particles. The potential term V_{12} couples the particles in the two groups. The standard Aziz potential[6]

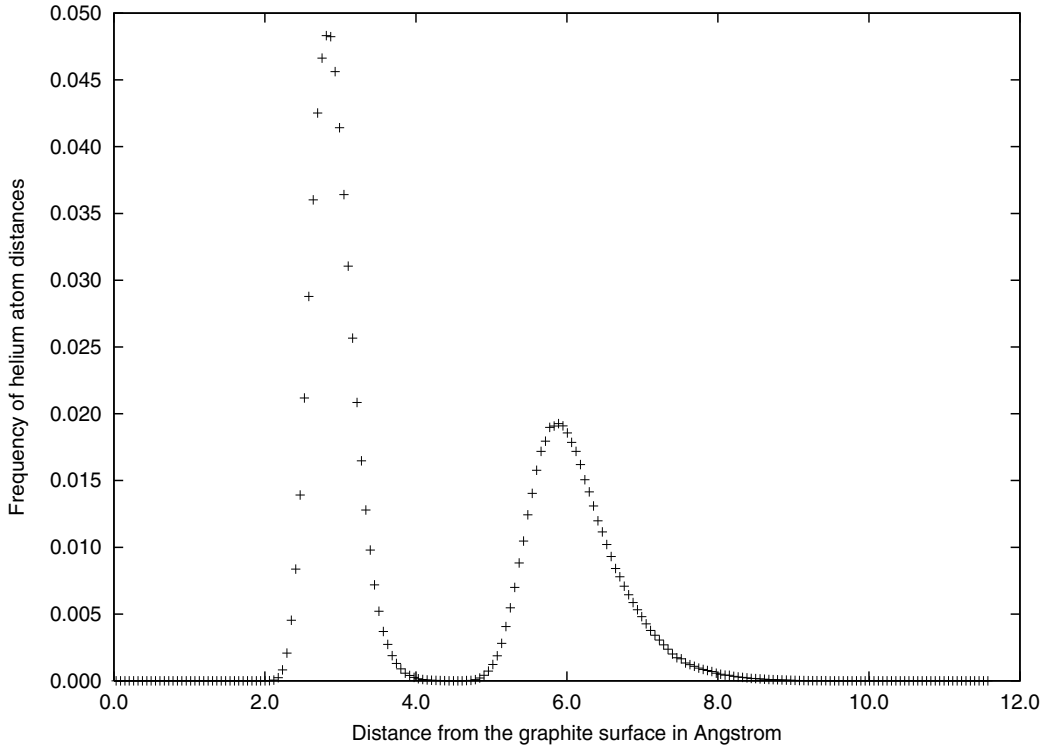

Figure 1. The average positions of the helium atoms from the simulation of the two layer helium film as a function of the distance from the graphite surface.

couples all the particles in the system. Our variational wave function is;

$$\Psi = \Psi_1 \Psi_2 J_{12} \, . \tag{3}$$

Here Ψ_1 and Ψ_2 are trial functions for each layer and are of the standard form[3]; a product of pair and triplet functions multiplied by a product of single particle functions. These single particle functions are taken to be the appropriate ground state functions for an atom in the effective potential for each layer. The Jastrow term J_{12} in our trial function correlates the atoms in the first and second layers. With the assumption that the N_1 and N_2 atoms form two layers it is reasonable to describe the localization in each layer by the appropriate single particle function. The values of N_1 and N_2 are of course at our disposal and determine the densities in the two layers. In our calculation we have not attempted to determine the equilibrium values of N_1 and N_2 by using a Monte Carlo algorithm designed to promote exchange of particles between the layers. With our standard algorithm particle exchange between the layers is possible but is not observed in long runs. In fact, the two layers are well defined and separated in all our calculations. Figure 1 presents the positions of all the helium atoms in the z direction, the distance from the graphite surface, in a simulation performed at a second layer density of 0.0888Å^{-2}. The value of N_1 varied between 100 and 144 particles; that for N_2 between 32 and 100 particles. In the simulation represented by Fig. 1, there were 128 helium atoms in the first layer and 98 atoms in the second layer.

The expectation value of Hamiltonian, Eq. (2), gives the total energy, E_{ML},

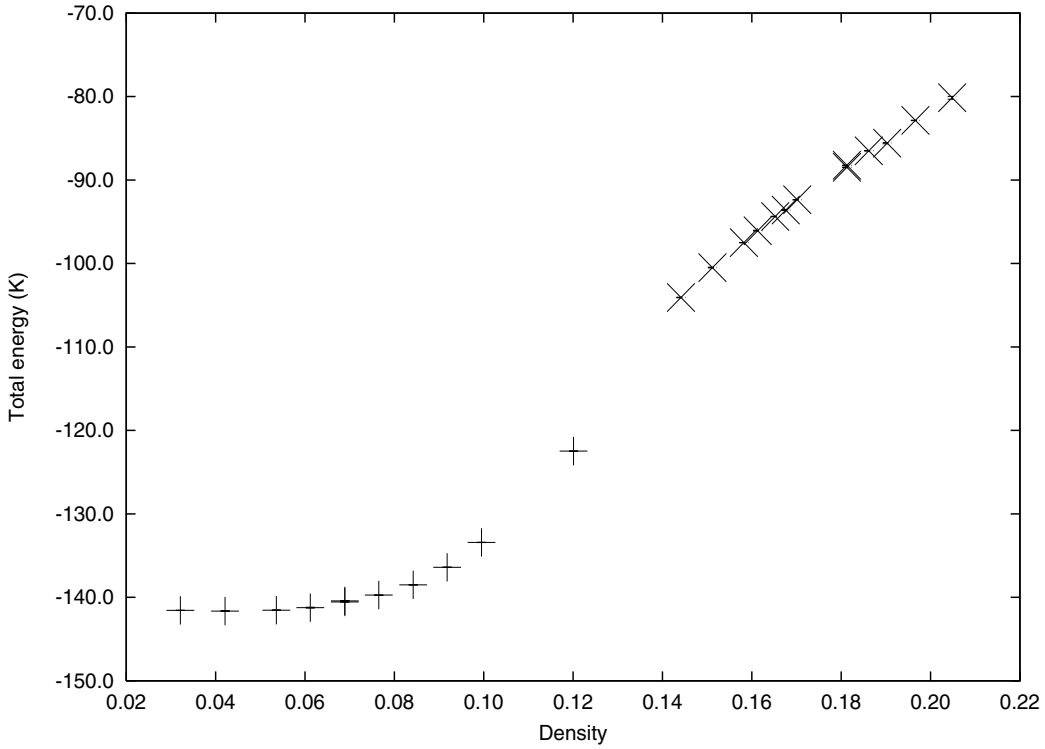

Figure 2. Total energy vs density from submonolayer densities to second layer completion. The monolayer energies are represented by (+) and the second layer total energies are shown by (X). The densities are in units of A^{-2}. The error bars on the energies are smaller than the symbol sizes.

of both the first and second layers and the interaction energy between them. This interaction energy consists of the expectation value of V_{12} and, in addition, the kinetic energy arising from the gradients of the coupling term J_{12}. The total energy can be directly compared with the total energy calculated in the submonolayer simulation as shown in Figure 2. However, it does not reveal any details of the behavior of the second layer atoms and can not be compared directly to the PEP energies. To facilitate such comparisons, it is useful to break up the total energy into two parts; the energy of the first layer and the energy of the second layer. This division is clearly not unique and our first estimator defines E_1 and E_2, the energies of the two layers, as follows,

$$E_1 =< H_1 > \tag{4}$$

$$E_2 =< H_2 > + < V_{12} > \ . \tag{5}$$

These expectation values are all computed with the full wave function given by Eq. (3). While this estimator resembles the approach proposed by Zhang and Kalos[9], there are fundamental differences. The random walks used to evaluate Eq. (2) were sampled from the full wavefunction and did not alternate between sampling Ψ_1 and Ψ_2. Thus both E_1 and E_2 contain expectation values of the appropriate gradient terms of J_{12}. We have added the expectation value of V_{12} to $< H_2 >$ because

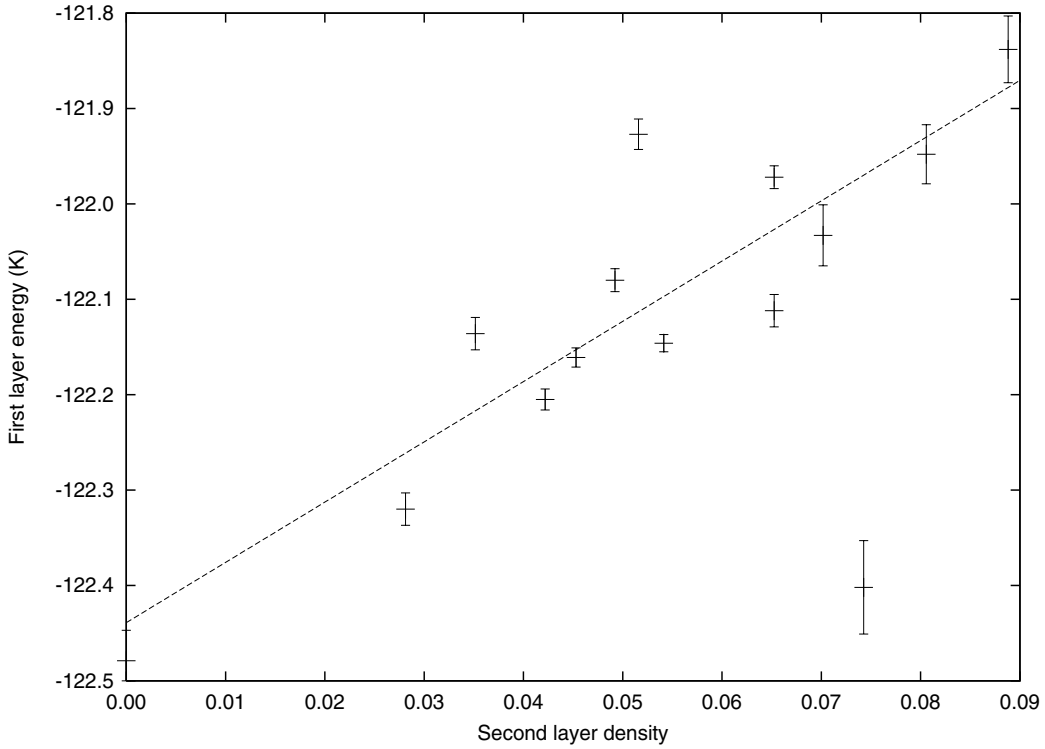

Figure 3. Change in the first layer energy given by Eq. (4) as the second layer completes. The second layer density is in units of A^{-2}.

our second layer PEP calculation contained an approximate treatment of this term. Equation (4) and (5) show explicitly how the configurations of the particles in one of the layers influence the energy of the other layer.

An alternative method of estimating the second layer energy uses the total energy, E_{ML} and the value of the total GFMC energy at monolayer completion, $E_M = -122.48(3)$. A difference estimator is given by:

$$E_2' = \frac{N * E_{ML} - N_1 * E_M}{N_2}\,, \tag{6}$$

where N is the total number of atoms in the system, and N_1 and N_2 are the number of atoms in the first and second layers, respectively. This estimator places all contributions to the energy from the gradient terms of J_{12} in the second layer energy. It can be expected that the E_2' energies will be higher than those from Eq. (5), but should show the same density dependence.

We performed our calculations with the density of the first layer fixed at 0.116 Å^{-2}. This is close to the completion density of the first layer. As the density of the second layer increases the first layer will be slightly compressed. We have ignored this small effect in the present calculation. However, E_1, as calculated by Eq. (4), is not fixed and varies with the second layer density. The energy now contains contributions from the gradients of J_{12}, and J_{12} also changes the Monte Carlo sampling. One expects that there will be less influence when the second layer is relatively dilute and more when it becomes dense. When the second layer has a density of 0.042 Å^{-2}

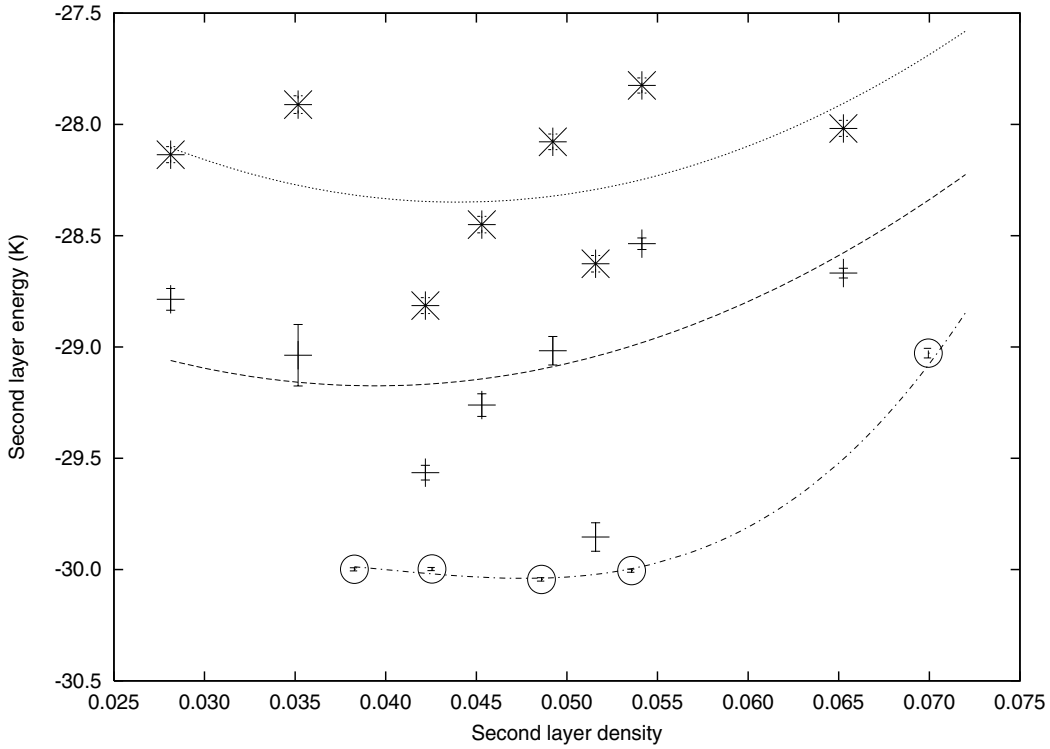

Figure 4. Second layer liquid phase energies as a function of density. The densities are in units of A^{-2}. The energies using Eq. (5), E_2, are shown by a (+) with an associated fitted curve given by (__). Those using Eq. (6), E_2', are represented by an (*) with a fitted curve given by a dashed line. The PEP energies are shown by a ◯ and the fit to Eq. (1) is shown by (_._.). The error bars on the energies are smaller than the symbol sizes for the PEP energies.

there is a 0.2% difference in the energy of the first layer when we compare E_1 to E_M. At a density of 0.081 Å^{-2} this difference increases to .43%. We regard both of these differences as small; the first layer is too dense to be significantly influenced by the second layer. However, the variance of E_1 is significant and affects the calculation of E_2. The variation of the first layer energy is shown in Figure 3. The line is a least squares fit to the energies and is provided as a guide to the eye. It turns out that nearly all of the energy change in the first layer arises from contributions to the kinetic energy from the gradients of the correlation J_{12}. If we omit this term the energy differences are less than 0.1%.

From the PEP simulations, it is clear that there are well-defined liquid and solid phases. In Figure 4, the energies for the second layer liquid phase from the PEP calculations and both estimators, E_2, Eq. (5) and E_2', Eq. (6), from the fully interacting first layer simulation are shown. As expected, the energies from Eq. (6) are consistently higher than those from Eq. (5). Also, the second layer energy estimators, E_2 and E_2', have significantly higher variances than those from the PEP simulations. It is clear that the kinetic energy contributed by the gradients of J_{12} are not modeled well by the passive effective potential. The second layer energies are higher from the fully interacting first layer estimators and the density at which the pressure is zero is lower than the PEP results. The zero pressure density from the energies calculated by

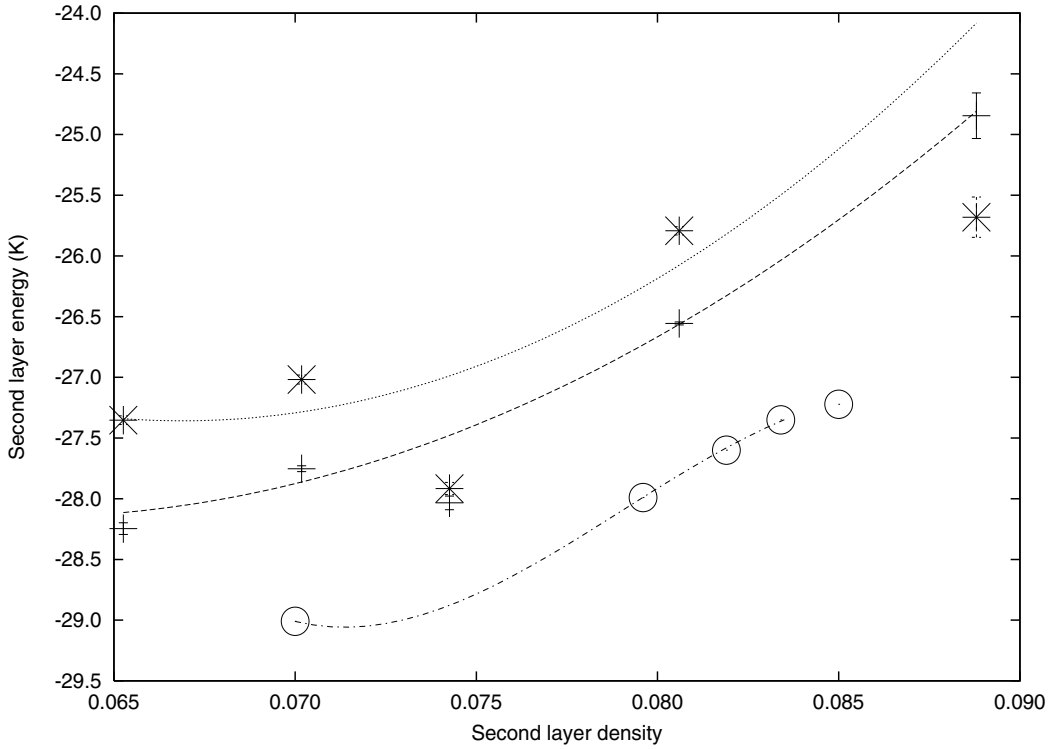

Figure 5. Second layer energies in the solid phase as a function of density. The densities are in units of A^{-2}. The energies using Eq. (5) are shown by a (+) with an associated fitted curve given by (__). Those using Eq. (6) are represented by an (*) with a fitted curve given by a dashed line. The PEP energies are shown by a ◯ and the fit to Eq. (1) shown by (_. _.). The error bars on the energies are smaller than the symbol sizes for most of the energies.

Eq. (6) occurs at 0.044Å. As mentioned above, this density from the PEP simulation was 0.048Å. Similar behavior for the second layer energy estimators is observed in the solid phase, shown in Figure 5. At most densities, the variance of the energies is less than in the liquid phase.

We now turn to a discussion of the chemical potential of the second layer. The chemical potential (μ) of the dilute second layer determines the completion density of the first layer. In I we calculated μ of the second layer using the same PEP as we have used in this paper and we also showed that varying the way in which the PEP was calculated changed the completion density by only a few percent. Our single particle calculation with a fully participatory first layer provides a more accurate value for μ; the value of -25.18K is about 4K higher than the PEP value. This small change causes a shift of 1% in the predicted completion density of the first layer, see Fig. 7 of I. For the second layer we have calculated, variationally, the energy (-25.18K $\pm$ 0.05) of a single helium atom when it interacts with all the atoms in the first layer. For this calculation, the Hamiltonian and wave function are of the form given by Eq. (2) and Eq. (3) but, with only a single particle in the second layer. Thus this single particle energy is different from that calculated from a PEP potential.

ACKNOWLEDGMENTS

We thank Silvio Vitiello for many useful discussions. One of us (P.A.W.) acknowledges support from DOD grant, No: N0014-96-1-1-1057 and travel support from the U.S. Army Research Office, Research Triangle Park, NC, through a grant administered by Southern Illinois University, Carbondale.

REFERENCES

[1] P. A. Crowell and J. D. Reppy, *Phys. Rev. B* **53**, 2701 (1996).

[2] C. E. Campbell, F. J. Milford, A. D. Novaco and M. Schick, *Phys. Rev A* **6**, 1648 (1972); B. E. Clements, E. Krotschek and H. J. Lauter, *Phys. Rev. Lett.* **70**, 1287 (1993).

[3] P. A. Whitlock, G. V. Chester and B. Krishnamachari, *Phys. Rev. B* **58**, 8704 (1998).

[4] P. A. Whitlock, G. V. Chester and B. Krishnamachari, *Comp. Physics Communications* **121-122**, 460 (1999).

[5] M. Pierce and E. Manousakis, *Phys. Rev. Lett.* **81**, 156 (1998).

[6] R. A. Aziz, V. P. S. Nain, J. S. Carley, W. L. Taylor and G. T. McConville, *J. Chem. Phys.* **70**, 4330 (1979).

[7] The effective potential used by Pierce and Manousakis[5] is different from ours. They assumed that the first layer was a static triangular lattice of helium atoms. This assumption leads to a periodic effective potential. The mean value of this potential, which is only a function of the distance from the first layer, is equal to the effective potential we use.

[8] R. A. Aziz, A. R. Janzen and M. R. Moldover, *Phys. Rev. Lett* **74**, 1586 (1995).

[9] S. Zhang and M. H. Kalos, *J. Stat. Phys.* **70**, 515 (1993).